ELSEVIER

Dyes and Pigments 49 (2001) 117–125

DYES and PIGMENTS

www.elsevier.com/locate/dyepig

Decolourization of textile industry wastewater by the photocatalytic degradation process

C. Hachem [1], F. Bocquillon, O. Zahraa, M. Bouchy *

Département de Chimie Physique des Réactions - UMIR 7630 CNRS ENSIC, 1, rue Grandville, BP 451, F-54001 - Nancy Cedex, France

Received 24 October 2000; received in revised form 4 December 2000; accepted 15 March 2001

Abstract

The photocatalytic degradation of various dyes (Orange II, Orange G, Congo Red, Indigo Carmine, Crystal Violet, Malachite Green, Remazol Blue and Methyl Yellow) has been studied, using P25 Degussa as catalyst. All dye solutions underwent a decolourization. The kinetics of reaction have been studied and were found to be zero or first order with respect to the dyes. This was compared with the adsorption properties. The effect of the addition of hydrogen peroxide has been studied. An enhancement of the rate has been observed in all cases and the order with respect to the additive was found to be almost zero. It is difficult to give a general picture of the kinetics using these very different dyes but the process was found to be effective for the decolourization of textile wastewater. © 2001 Published by Elsevier Science Ltd.

Keywords: Dyes; Decolourization; Photocatalysis; Kinetics; Hydrogen peroxide; Textile industry

1. Introduction

Textile industry wastewater is heavily charged with unconsumed dyes, surfactants and sometimes traces of metals. These effluents cause a lot of damage to the environment. In most countries researchers are looking for appropriate treatments in order to remove pollutants, impurities and to obtain the decolourization of dyehouse effluents [1–3]. Various chemical and physical processes are currently used, which work by direct precipitation and separation of pollutants [4], or elimination by adsorption on activated carbon or similar materials. In this case, the problem is only displaced, and further treatments are indeed necessary in order to separate the purified effluents or to regenerate the adsorbents; therefore, a new and different risk of pollution is faced [5]. Alternatively, a photochemical approach has been adopted. Indeed, ultraviolet irradiation combined or not with oxidative agents such as ozone or hydrogen peroxide leads to a complete destruction of the pollutants [6–9], but the presence of intermediates arising from the photodegradation reaction could be more harmful than the pollutant itself [10,11]. Such inconvenience can be avoided by using the photocatalytic degradation. In this process, hydroxyl radicals (OH°) are

* Corresponding author.

E-mail addresses: michel.bouchy@ensic.inpl-nancy.fr (M. Bouchy), orfan.zahraa@ensic.inpl-nancy.fr (O. Zahraa).

[1] Present address: Chemistry Department, Faculty of Sciences, Damascus University.

0143-7208/01/$ - see front matter © 2001 Published by Elsevier Science Ltd.
PII: S0143-7208(01)00014-6

generated when the photocatalyst is illuminated in the presence of water and air [12–14], these ultra reactive species associated with oxygen are able to achieve a complete mineralization of organic pollutants into carbon dioxide, water and other non-toxic products [15,16].

The aim of this study is to analyse the kinetics of decolourization of various types of dyes and to assess the influence additives have on the process.

2. Experimental procedures

2.1. Materials

The dyes Orange II, Orange G, Congo Red, Indigo Carmine, Crystal Violet, Malachite Green, Remazol Blue and Methyl Yellow were commercial products purchased from Sigma Chemical Co., and used without further purification (see Fig. 1). Hydrogen peroxide (30%, w/w) was obtained from Fluka. Purified water was obtained from an Elix Millipore equipment. The titanium dioxide used, "TITANDIOXID P25" Degussa, was about 70% anatase. According to the manufacturer's specifications [17], the elementary particle in dry powder was approximately spherical in shape with a size of 20 nm. The specific surface area, as measured by N_2 adsorption at 77 K, was 44 $m^2\ g^{-1}$ [18].

The experimental set-up for the photocatalytic decolourization has been described previously [19]. The photocatalyst has been deposited on 3.8×48 cm^2 glass plates from a suspension of TiO_2.

2.2. Procedure

A suspension of commercial Degussa P25 TiO_2 of 4 g l^{-1} in pure water was prepared, the pH was adjusted to about 3 and it was sonicated. A given volume suspension was carefully poured on the glass plate and allowed to dry out at 100°C for a few hours.

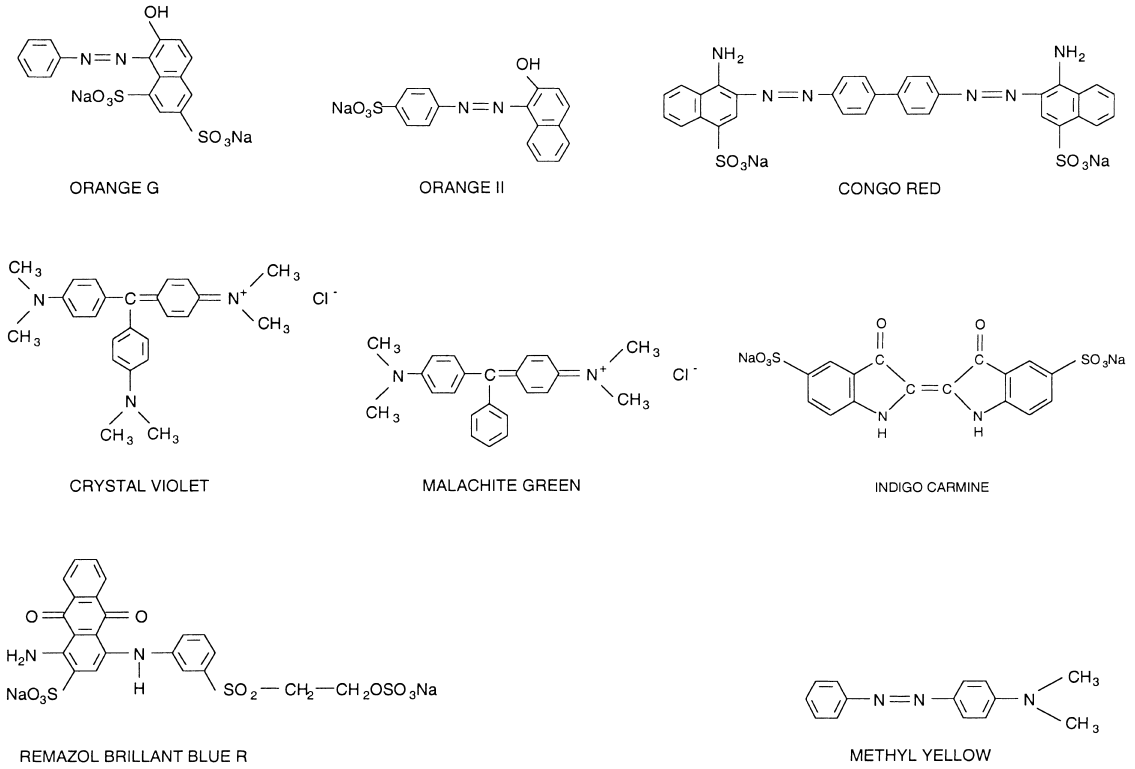

Fig. 1. Developed formulae of various dyes used in this study.

After drying, the plate was fired at 475°C for 4 h (Fig. 2). During the heating, OH groups from the catalyst surface and the support can react and lose a molecule of water, creating an oxygen bridge, thus increasing the adherence of the catalyst to the support. Before deposition, the glass surface was treated using a dilute acid solution of HF and washed in a basic solution of NaOH in order to increase the number of OH groups. The suspension concentration 4 g l^{-1} was chosen so as to get thin enough deposits. This deposition process was carried out four times in succession so as to increase the total thickness. As shown in Fig. 3, the first coat does not cover all the surface but additional coats lead to a complete coverage.

After each run, the catalyst was washed and irradiated for several hours in the presence of H_2O_2 so that it was regenerated.

Electron microscopy was carried out on a Jeol T33OA scanning microscope with the help of the LSGC Laboratory. Profilometry measurements were carried out on a UBM optical profilometer equipped with a MICROFOCUS probe. Fig. 4 shows the topology of a TiO_2 deposit which shows a uniform surface of roughness of about 5 μm. In addition, the average thickness was estimated to be 10 μm [20]. BET areas were determined on a FISON Sorptomatic 1900 sorptometer.

Photocatalytic measurements were carried out on a homemade reactor designed for testing 3.8× 48 cm^2 flat glass plates carrying the deposited film of catalyst (Fig. 5). The total volume of aqueous solution was 0.2 l. The solution was continuously circulated with a peristaltic pump, flowing freely over the catalytic surface and stirred in the 0.1 l tank and could be considered as being constantly air-equilibrated. The circulating flow was 0.4 l min^{-1}.

As the extent of adsorption or photocatalytic degradation was very small during a single pass (0.5 min), the whole system could be considered as a perfectly stirred sealed reactor with respect to the solution. Irradiation of the photocatalyst was carried out by a MAZDA-TFN18 18 W UV fluorescent lamp emitting around 365 nm and positioned parallel to the plate. The average flux on the plate was estimated to be about 2.10^{-3} E min^{-1} m^{-2} [20]. Adsorption measurements were made using the same set-up in the absence of irradiation.

Absorption measurements to monitor the dye concentration in the aqueous phase were carried out on a Lambda-2 Perkin-Elmer UV/vis spectrophotometer.

3. Results and discussion

The kinetics of photocatalytic degradation of the various dyes are pictured in Fig. 6a–g, as the decrease in the relative concentration C/C° of the dye with the time of irradiation, where C is the running concentration and C° the concentration at the beginning of the irradiation. Note that the solution

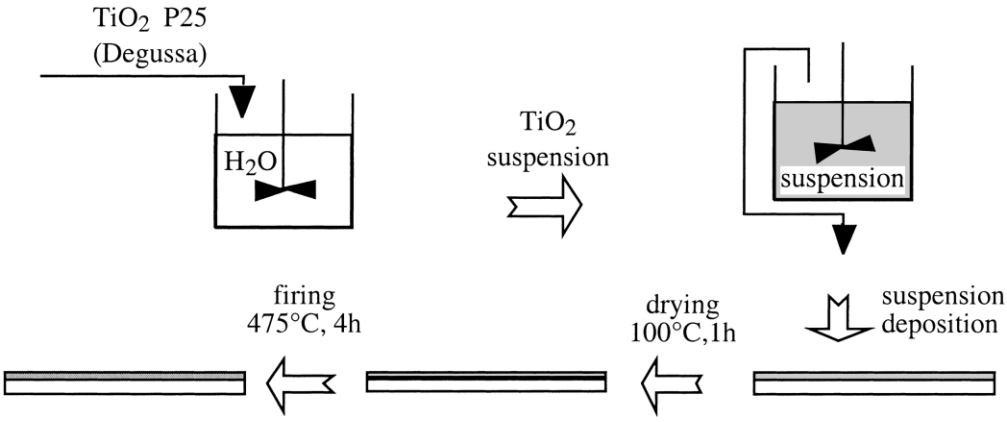

Fig. 2. Procedure for the preparation of the TiO_2 deposits.

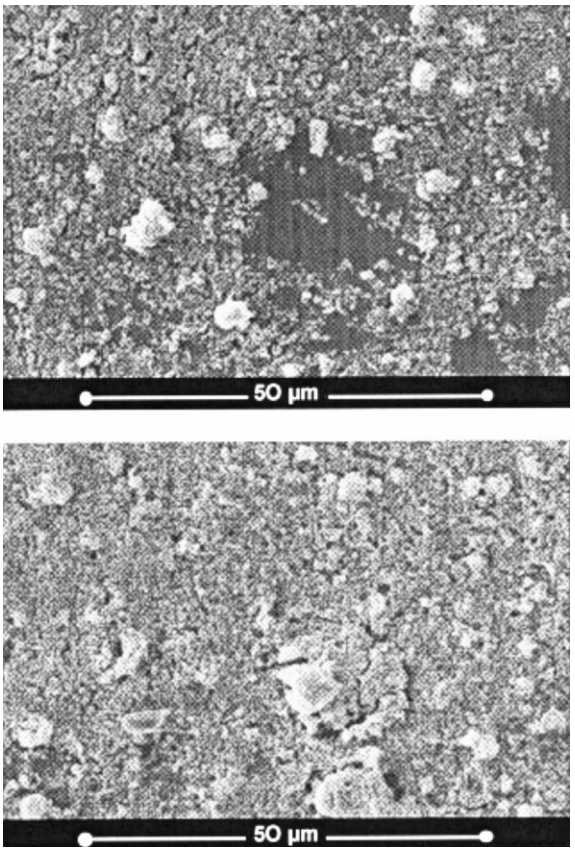

Fig. 3. Electron micrographs of P25 deposits (top: first coat; bottom: 4 coats).

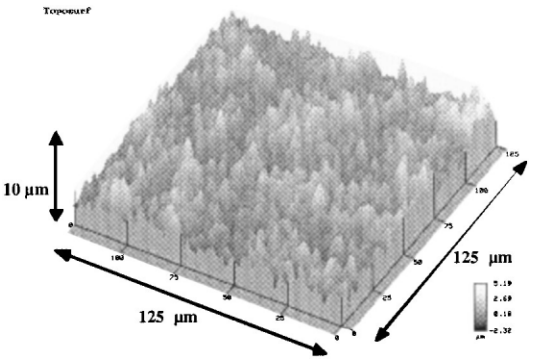

Fig. 4. Profilogram of a TiO_2 deposit.

was allowed to equilibrate with the catalyst prior to irradiation so that C° is lower that the actual initial concentration of the sample C_i. A typical experiment is given in Fig. 7.

3.1. Adsorption on the catalyst

As a rule, adsorption was quite fast and the equilibrium concentration C° was reached within about 45 min. The contact was carried out up to 90 min, but no significant change in the concentration was observed.

Although the initial concentrations of the various dyes were comparable, the equilibrium value for C° varied indicating different adsorption properties. The fraction of dye adsorbed was expressed as $A=(C_i-C^\circ)/C_i$ as given in Table 1.

Acid dyes, Orange II, Orange G, Remazol Blue and Indigo Carmine exhibited a low adsorption and in most cases A was not measurable (within the experimental error of about 0.02). Alternatively, cationic dyes, Malachite Green and Crystal Violet were easily adsorbed. This difference can be attributed to a higher solvation energy for acid dyes. The sulphonate group can indeed allow the formation of hydrogen bonds contrary to the quaternary amines of the cationic dyes [21]. As a consequence, the equilibrium between the adsorbed and the solvated forms is more in favour of the adsorption for the cationic than the acid dyes. The pH is about 5.5, and, therefore, is close to the isoelectric pH of 5.8 [22] where the solid surface has a neutral global charge; there is then little segregation according to the charge of the ions. The direct dye Congo Red, which possesses sulphonate groups, exhibited a high adsorption ($A=0.1$), which can be attributed to both the high molecular weight of this molecule compared to the other acid, and the large hydrophobic middle section.

At a very acid pH, the acid dyes are in neutral form, which is less hydrophilic than the ionic form, and adsorb strongly. For example, at pH 1.3, Orange II undergoes a fast and strong adsorption leading to a visible colourization of the catalyst. Under these conditions, practically no photocatalytic degradation was observed, which was attributed to a complete coverage of the surface. This indeed prohibits the adsorption of H_2O or OH^- on the surface, and inhibits the initial process of formation of the reactive hydroxyl radicals.

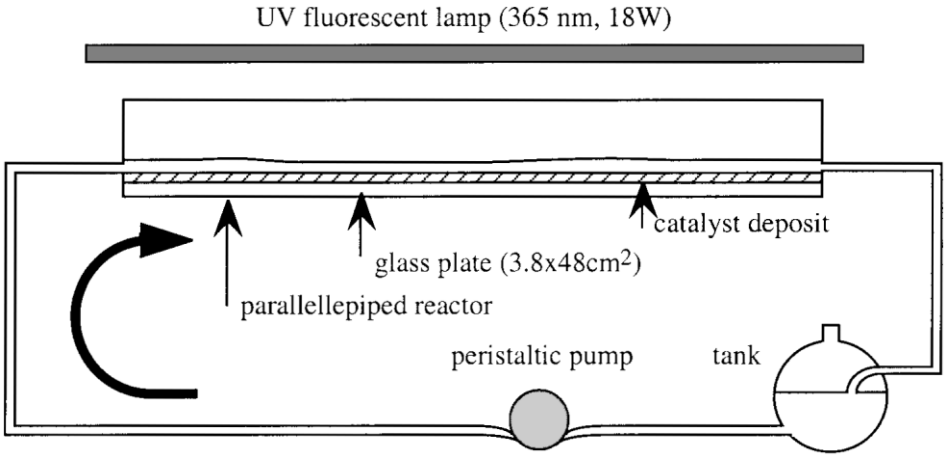

Fig. 5. Experimental set-up for reactant adsorption and photocatalytic degradation.

3.2. Kinetics of photocatalytic degradation

The rate of photocatalytic degradation was determined as the rate of disappearance of the dye. This degradation also is the decolourization process, as the possible intermediates formed did not absorb in the visible range. The disappearance was, therefore, followed by absorption in the visible range. The rate of degradation was expressed as the intrinsic rate relatively to the area of deposit (i.e. the area of the glass support) under given conditions of catalyst load (12.5 g m^{-2}) and intrinsic light flux (2.0 10^{-3} E min^{-1} m^{-2}); the rate was then expressed in units of mol min^{-1} $m^{-2}_{deposit}$. This is of practical interest in designing a photoreactor as doubling the irradiated deposited area doubles the rate of degradation in the reactor. Note that this deposit area is not to be mistaken with the much larger catalyst surface area. The kinetics were found to be of order 0 or 1 with respect to the dye. Plotting either C/C° or ln (C/C°) versus time checked the validity of the order. Discriminating between the two orders requires an extent of reaction higher than 0.3, which is not always the case. When the extent was small, the order has been assumed to be the same as in experiments carried out in the presence of H_2O_2 as an accelerating agent. It can be verified indeed in the case of fast degradations that the order was not altered in the presence of this agent.

These orders can be considered to be associated with the limiting cases of the common Langmuir–Hinshelwood model. In this simple model the rate r is expressed as [14,23]:

$$r = k \cdot \left[\frac{KC}{1 + KC} \right]$$

where k is a rate constant (function of the light flux) and K the adsorption constant. At low adsorption, r is equal to kKC (order 1) and at high adsorption, r is equal to k (order 0).

However, no correlation between the adsorption and the order can be found in the results given in Table 1. For example, low adsorption dyes, Orange II and Orange G, have an order of 1 and 0 respectively. This can arise from the existence of specific reactive sites on the surface; these could be associated with efficient traps favouring the formation of a reactive hydroxyl radical. If these sites are relatively few with respect to all the sites, the total adsorption does not reflect the adsorption on these specific sites. Therefore, there may be a stronger "effective" adsorption of Orange G compared to Orange II. According to the LH model, the rate would reach a maximum value at high adsorption (order 0). However, the rate for Orange G is lower than the rate for Orange II. This discrepancy could be attributed to a different reactivity, which is expressed by the rate constant k. The fragile group

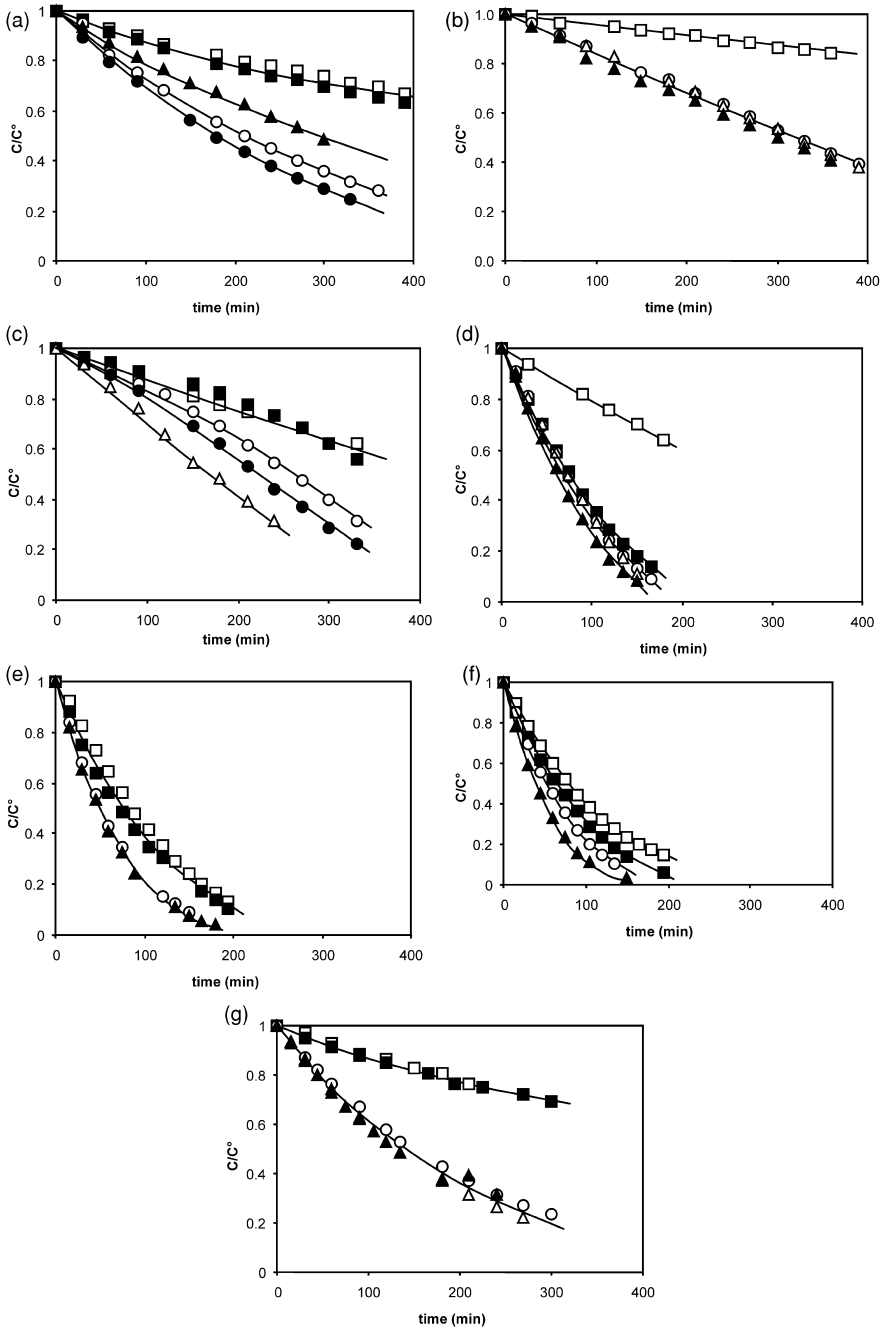

Fig. 6. (a) Photocatalytic degradation of Orange II following dark adsorption (□ $C^{\circ} = 9.9\ 10^{-5}$ mol l^{-1}, irradiation flux 7 10^{-7} E min^{-1}); effect of H_2O_2 (■ 10^{-3} mol l^{-1}, ○ 10^{-2} mol l^{-1}, ● 2 10^{-2} mol l^{-1}, △ 5 10^{-2} mol l^{-1}, ▲ 10^{-1} mol l^{-1}). (b) Photocatalytic degradation of Orange G ($C^{\circ} = 9.9\ 10^{-5}$ mol l^{-1}), same conditions as in Fig. 6a. (c) Photocatalytic degradation of Congo Red ($C^{\circ} = 3.5\ 10^{-5}$ mol l^{-1}), same conditions as in Fig. 6a. (d) Photocatalytic degradation of Indigo Carmine ($C^{\circ} = 9.5\ 10^{-5}$ mol l^{-1}), same conditions as in Fig. 6a. (e) Photocatalytic degradation of Crystal Violet ($C^{\circ} = 1.8\ 10^{-5}$ mol l^{-1}), same conditions as in Fig. 6a. (f) Photocatalytic degradation of Malachite Green ($C^{\circ} = 1.9\ 10^{-5}$ mol l^{-1}), same conditions as in Fig. 6a. (g) Photocatalytic degradation of Remazol Blue ($C^{\circ} = 9.6\ 10^{-5}$ mol l^{-1}), same conditions as in Fig. 6a.

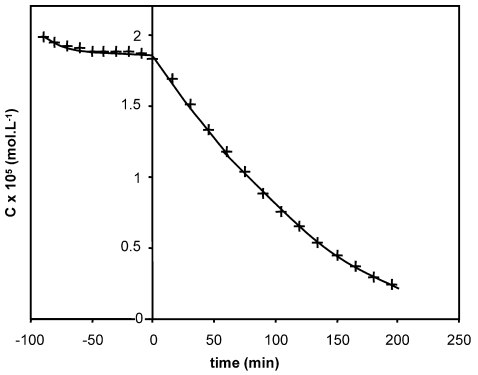

Fig. 7. Variation of the dye concentration vs. time, showing the dark adsorption ("negative time") followed by the irradiation at time $t = 0$ (Crystal Violet).

in these dyes is the NH group, which results from an equilibrium between two tautomeric forms [21] where an H atom is exchanged between O and N as shown in Fig. 8. This equilibrium is much influenced by the electron-attracting sulphonate groups, which would result in an enhancement in the amine form in the case of Orange II. Accordingly, although the adsorption is lower for this dye, a high reactivity leads to a higher rate of photocatalytic degradation compared with Orange G. This shows the difficulty in comparing the photocatalytic degradability of the various dyes.

Cationic dyes exhibit a relatively high adsorption but the rate of degradation is only twice that of the low adsorbing Orange II. Moreover, according to an order of the unity with respect to the dye, the rate of degradation of the cationic dyes would be higher at the initial concentration of the acid dyes (10^{-4} mol l^{-1}). However, both adsorption and reactivity play a role in the global kinetics. It is probable that the azo group is more likely to be attacked via the abstraction of H on the NH form by the reactive species, assumed to be the hydroxyl radical, than the phenyl groups via addition. The reactivity of Remazol Blue can also be attributed to the presence of an NH group.

The dispersed dye Methyl Yellow has a very low solubility in water. Solvents such as methanol and dimethylformamide have been used in order to get a homogeneous solution. A very high rate of decolourization was then observed, which suggests a process involving the additional solvent, but this was not further studied, as the addition of the organic solvent cannot be envisaged in an industrial process.

3.3. Limiting processes

It is of interest to compare the rate of adsorption r_a with the rate of degradation r°. This rate r_a

Table 1
Properties and kinetics parameters of various dyes

Dye	Orange II	Orange G	Congo Red	Indigo Carmine	Crystal Violet	Malachite Green	Remazol Blue	Methyl Yellow
Class	Acid	Acid	Direct	Acid	Cationic	Cationic	Reactive	Dispersed
Type	Azo	Azo	Diazo	Carbonyl	Triphenyl	Triphenyl	Quinon	Azo
Color index	15,510	16,230	22,120	73,015	42,555	42,000	61,200	11,020
λ_{max} (nm)	485	480	498.5	610	590	617	595	448
Initial concentration C_i (mol l^{-1})$\times 10^5$	8.9	9.9	3.9	9.7	2.0	2.0	9.6	
A	<0.02	<0.02	0.1	~ 0.02	0.1	0.06	<0.02	–
Initial rate of deg radiation r° (mol min^{-1} m^{-2})$\times 10^5$	1.07	0.42	0.38	1.84	1.90	1.92	1.04[a]	13.44[b]
Order/dye	1	0	0	0	1	1	0	–
$r^\circ_{H_2O_2}/r^\circ$[c]	2.8	3.7	2	7	1.4	1.5	4.6	–
Order/H_2O_2	>0	0	>0	0	>0	>0	>0	–
ε (l mol^{-1} cm^{-1})$\times 10^{-5}$	4.48	0.23	0.49	0.22	0.92	0.86	0.13	–

[a] pH = 2.85.
[b] Average degradation rate over 150 min.
[c] $(H_2O_2) = 10^{-2}$ mol l^{-1}.

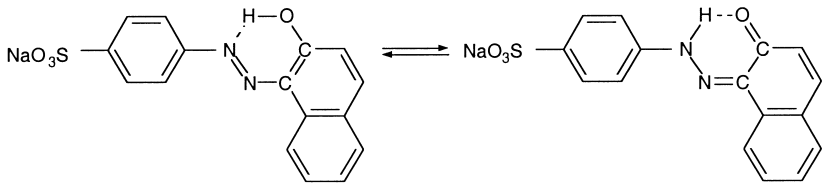

Fig. 8. Equilibrium between the two tautomeric forms in the acid dye Orange II.

can only be estimated if the amount of adsorption is large enough to allow a measurable decrease in the dye concentration in the aqueous solution. This is the case of half the dyes only. As the reaction of degradation follows the adsorption, the initial rate r° is necessarily lower than the initial rate $r_a{}^\circ$. This is effectively the case in Congo Red where the ratio $r^\circ/r_a{}^\circ$ is equal to about 0.4 but the situation is the reverse in the case of the cationic dyes where $r^\circ/r_a{}^\circ$ is equal to about 2.5 and 6.5 for Crystal Violet and Malachite Green, respectively. This infers that the adsorption process involved in the degradation is much faster than the adsorption monitored prior to irradiation. This could be due the existence of different types of sites as suggested above or to an enhancement of the adsorption rate in the presence of irradiation. Another important process involved in the mechanism is the transport process. This latter is very fast: as an example, when a rapid adsorption takes place for Orange H in acid medium, the initial rate is noticeably higher than the largest degradation rate observed for the most reactive dyes in the presence of H_2O_2.

3.4. Effect of H_2O_2

Usually this additive is known to increase the rate of photocatalytic degradation by allowing an enhancement in the quantum yield of formation of hydroxyl radical [24,25]. This is observed indeed for all dyes in the present study as shown in Fig. 9. In most cases, a limiting rate is reached when increasing the additive concentration, so that there is little change between the addition of 10^{-2} or 10^{-1} mol l^{-1}. Addition of a concentration of 10^{-3} mol l^{-1} is generally not sufficient to increase the rate significantly. Consequently, the effect of the additive has been given in Table 1 as the factor of increase in the initial rate when using a concentration of 10^{-2} mol l^{-1}.

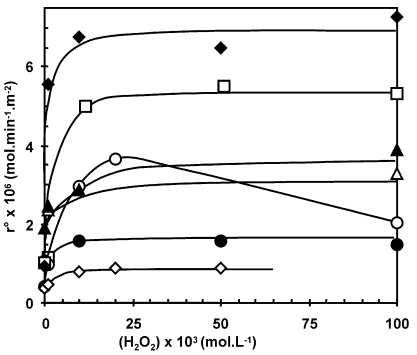

Fig. 9. Effect of the addition of H_2O_2 on the initial rate r° of degradation of the dyes (conditions as in Table 1); ○ Orange II, ● Orange G, ◇ Congo Red, ◆ Indigo Carmine (× 1/2), △ Crystal Violet, ▲ Malachite Green, □ Remazol Blue.

The picture above is a general trend. However, some dyes exhibit a slight difference. For example, Congo Red, Orange II and Malachite Green do exhibit a slightly positive order with respect to H_2O_2 in the range 10^{-2}–10^{-1} mol l^{-1}. The case of Orange II is of special interest as the rate goes through a maximum when increasing the concentration of the additive. This effect could be due to a competition for adsorption between the dye and the additive. This is in agreement with a low adsorption of this dye as suggested above.

Addition of H_2O_2 does not seem to alter the basic kinetics, as the order with respect to the dye is not modified. The effect could only be due to an increase in the OH° radical formation. This suggests a similar limiting value of the rate of decolourization of the various dyes at high additive concentration. This ideal case is not strictly observed. However, it can be seen from Table 1 that the lower the intrinsic rate, the higher it is increased by the additive. Indigo Carmine is a noticeable exception to this rule.

4. Conclusion

The photocatalytic process has proved very effective in decolourizing aqueous solutions of the various textile dyes. As both adsorption and reactivity play a role in the kinetics, it is difficult to get a satisfactory general picture of the mechanism. Comparing degradation and adsorption suggests that the degradation takes place on specific types of adsorption sites on the catalyst surface. The order with respect to the dye is either zero or one, which may be in relation with a limiting adsorption on the active sites. The addition of hydrogen peroxide enhances the rate of degradation, which is of much interest for improving the quantum yield of degradation. Finally, it is to be noted that the irradiation used falls within the UV range available from the sun, which suggests the design of a solar photoreactor for a decolourization process in regions where much solar energy is available.

References

[1] Galindo C, Jacques P, Kalt A. Photodegradation of the aminobenzene acid orange 52 by three advanced oxidation processes: UV/H_2O_2, UV/TiO_2 and VIS/TiO_2 comparative mechanistic and kinetic investigations. J Photochem Photobiol A: Chem 2000;130:35–47.

[2] Akmehmet Balcioglu I, Arslan I. Treatment of textile industry wastewater by enhanced photocatalytic oxidation reaction. J Adv Oxid Technol 1999;4:189–95.

[3] Porada T, Gade R, Faβler D, Günther K. Quatum yield of TiO_2-photocatalysed degradation of Acid Orange 7. J Adv Oxid Technol 1999;4:203–8.

[4] Wu J, Eiteman MA, Law SE. Evaluation of membrane filtration and ozonation processes for treatment of reactive dye wastewater. J Environ Eng 1998;124:272–7.

[5] Hoffmann MR, Martin ST, Choi W, Bahnemann D. Environmental applications of semiconductor photocatalysis. Chem Rev 1995;95:69–96.

[6] Majcen-Le Marechal A, Slokar YM, Taufer T. Decoloration of chlorotriazine reactive azo dyes with H_2O_2/UV. Dyes and Pigments 1997;33:281–8.

[7] Galindo C, Kalt Y, Taufer A. UV/H_2O_2 oxidation of azodyes in aqueous media: evidence of a structure–degradability relationship. Dyes and Pigments 1999;42: 199–207.

[8] Kuo W. Decolorizing dye wastewater with Fenton's reagent. Wat Res 1992;26:881–6.

[9] Zhang F, Zhao J, Shen T, Hidaka H, Pelizetti E, Serpone N. TiO_2-assisted photodegradation of dye pollutants II. Adsorption and degradation kinetics of eosin in TiO_2 dispersions under visible light irradiation. Appl Cat B: Environ 1998;15:147–56.

[10] Anderson MA, Yamazaki-Nishida S, Cervera-March S. In: Ollis DF, Al-Ekabi H, editors. Photocatalytic purification and treatment of water and air. Amsterdam: Elsevier; 1993. p 405–20.

[11] Larson SA, Falconer J. In: Ollis DF, Al-Ekabi H, editors. Photocatalytic purification and treatment of water and air. Amsterdam: Elsevier; 1993. p. 473–9.

[12] Matthews RW. Photooxidation of organic impurities in water using thin films of titanium dioxide. J Phys Chem 1987;91:3328–33.

[13] Fox MA. Photocatalysis: decontamination by sunlight. Chemtech 1992:680–96.

[14] Chen HY, Zahraa O, Bouchy M, Thomas F, Bottero JY. Adsorption properties of TiO_2 related to the photocatalytic degradation of organic contaminants of water. J Photochem Photobiol A: Chem 1995;85:179–86.

[15] Tunesi S, Anderson M. Influence of chemisorption on the photodecomposition of salicylic acid and related compounds using suspended TiO_2 ceramic membrane. J Phys Chem 1991;95:3399–405.

[16] Matthews RW, McEvoy SR. A comparison of 254 nm and 350 nm excitation of TiO_2 in simple photocatalytic reactors. J Photochem Photobiol A: Chem 1992;66:355–66.

[17] Degussa Corp. Technical bulletin pigments, No. 56. 5th ed. Degussa AG, Frankfurt; 1990.

[18] Chen HY, Zahraa O, Bouchy M. Inhibition by inorganic ions of the adsorption and the photocatalytic degradation of organic contaminants in TiO_2 aqueous suspension. J Photochem Photobiol A: Chem 1997;108:37–44.

[19] Zahraa O, Dorion C, Ould-Mame SM, Bouchy M. Titanium dioxide deposit films for photocatalytic studies of water pollutants. J Adv Oxid Technol 1999;4:40–6.

[20] Ould-Mame SM. Etude de catalyseurs déposés pour réacteur photocatalytique de traitement des eaux. PhD thesis. Nancy, INPL. 1998.

[21] Galindo C, Jacques P, Kalt A. Total mineralization of an azo dye [Acid Orange 7] by UV/H_2O_2 oxidation. J Adv Oxid Technol 1999;4:400–7.

[22] Zahraa O, Chen HY, Bouchy M. Photocatalytic degradation of 1,2-dichloroethane on suspended TiO_2. J Adv Oxid Technol 1999;4:167–73.

[23] Mills A, Davies R. In: Ollis DF, Al-Ekabi H, editors. Photocatalytic purification and treatment of water and air. Amsterdam: Elsevier; 1993. p. 595–600.

[24] Salvador P, Decker F. On the generation of H_2O_2 during water photoelectrolysis at n-TiO_2. J Phys Chem 1984; 88:6116–20.

[25] Jenny B, Pichat P. Determination of the actual photocatalytic rate of H_2O_2 decomposition over suspended TiO_2. Fitting to the Langmuir–Hinshelwood form. Langmuir 1991;7:947–54.